OXFORD

Human Molecular Genetics, 2022, Vol. 31, 9, 1519–1530
https://doi.org/10.1093/hmg/ddab337
Advance access publication date 20 November 2021
General Article

Dorsal telencephalon-specific *Nprl2*- and *Nprl3*-knockout mice: novel mouse models for GATORopathy

Saeko Ishida[1,2,†,*], Di Zhao[1,2,†], Yuta Sawada[1], Yuichi Hiraoka[1,3], Tomoji Mashimo[2] and Kohichi Tanaka[1,4]

[1]Laboratory of Molecular Neuroscience, Medical Research Institute (MRI), Tokyo Medical and Dental University (TMDU), Tokyo, 113-8510, Japan
[2]Division of Animal Genetics, Laboratory Animal Research Center, The Institute of Medical Science, The University of Tokyo, Tokyo, 108-8639, Japan
[3]Laboratory of Genome Editing for Biomedical Research, MRI, TMDU, Tokyo, 101-0062, Japan
[4]Center for Brain Integration Research (CBIR), TMDU, Tokyo, 113-8510, Japan
*To whom correspondence should be addressed at: Division of Animal Genetics, Laboratory Animal Research Center, The Institute of Medical Science, The University of Tokyo, Tokyo, 108-8639, Japan. Tel: +813-6409-2489; Fax: +813-6409-2226; Email: saeishida@ims.u-tokyo.ac.jp
†Contributed equally.

Abstract

The most frequent genetic cause of focal epilepsies is variations in the GAP activity toward RAGs 1 complex genes DEP domain containing 5 (*DEPDC5*), nitrogen permease regulator 2-like protein (*NPRL2*) and nitrogen permease regulator 3-like protein (*NPRL3*). Because these variations are frequent and associated with a broad spectrum of focal epilepsies, a unique pathology categorized as GATORopathy can be conceptualized. Animal models recapitulating the clinical features of patients are essential to decipher GATORopathy. Although several genetically modified animal models recapitulate *DEPDC5*-related epilepsy, no models have been reported for *NPRL2*- or *NPRL3*-related epilepsies. Here, we conditionally deleted *Nprl2* and *Nprl3* from the dorsal telencephalon in mice [*Emx1*$^{cre/+}$; *Nprl2*$^{f/f}$ (*Nprl2*-cKO) and *Emx1*$^{cre/+}$; *Nprl3*$^{f/f}$ (*Nprl3*-cKO)] and compared their phenotypes with *Nprl2*$^{+/-}$, *Nprl3*$^{+/-}$ and *Emx1*$^{cre/+}$; *Depdc5*$^{f/f}$ (*Depdc5*-cKO) mice. *Nprl2*-cKO and *Nprl3*-cKO mice recapitulated the major abnormal features of patients—spontaneous seizures, and dysmorphic enlarged neuronal cells with increased mechanistic target of rapamycin complex 1 signaling—similar to *Depdc5*-cKO mice. Chronic postnatal rapamycin administration dramatically prolonged the survival period and inhibited seizure occurrence but not enlarged neuronal cells in *Nprl2*-cKO and *Nprl3*-cKO mice. However, the benefit of rapamycin after withdrawal was less durable in *Nprl2*- and *Nprl3*-cKO mice compared with *Depdc5*-cKO mice. Further studies using these conditional knockout mice will be useful for understanding GATORopathy and for the identification of novel therapeutic targets.

Introduction

Focal epilepsy, in which seizures arise from a single brain region, accounts for 60% of all epilepsies (1). The role of genetic factors is increasingly recognized. The *DEPDC5* (HGNC#18423; OMIM#614191) gene is one of the most frequent causes of focal epilepsy. Heterozygous loss-of-function *DEPDC5* mutations have been reported in various types of sporadic and inherited focal epilepsies, such as familial focal epilepsy with variable foci (FFEVF; OMIM#604364) (2,3), autosomal dominant nocturnal frontal lobe epilepsy (ADNFLE; OMIM#600513) (3) and familial temporal lobe epilepsy (FTLE; OMIM#600512) (3). A fraction of patients shows cortical malformation, such as hemimegalencephaly and focal cortical dysplasia (FCD) (4–6). FCD type 2, characterized by dysmorphic neurons and balloon cells, is one of the most common causes of pediatric refractory epilepsies, and 52% of *DEPDC5*-related epilepsies with FCD are drug-resistant (7). In addition, the variations in *DEPDC5* are also linked to an increased risk of sudden unexpected death in epilepsy (SUDEP) (7). Animal models revealed that homozygous knockout of *Depdc5* (*Depdc5*$^{-/-}$) in rodents leads to global growth delay and severe phenotypic defects that are embryonic lethal (8,9). Although heterozygous knockout (*Depdc5*$^{+/-}$) rodents are viable, they show neither spontaneous seizures nor increased susceptibility to seizure. Recent clinical studies using brain specimens of *DEPDC5*-related epilepsy patients with FCD revealed the existence of somatic second-hit loss-of-heterozygosity in the seizure-onset zone (6,10). This indicates that a biallelic two-hit brain somatic and germline-mutational mechanism causes a functionally homozygous knockout condition that may be responsible for the pathogenesis. This 'two-hit' hypothesis has also been supported by studies using mouse models in which *Depdc5* is knocked out in a limited brain region (10–13).

DEPDC5 is a subunit of the GAP activity toward RAGs 1 (GATOR1) complex. GATOR1 is a repressor of the

Received: September 28, 2021. **Revised:** September 28, 2021. **Accepted:** November 12, 2021
© The Author(s) 2021. Published by Oxford University Press. All rights reserved. For Permissions, please email: journals.permissions@oup.com
This is an Open Access article distributed under the terms of the Creative Commons Attribution Non-Commercial License (https://creativecommons.org/licenses/by-nc/4.0/), which permits non-commercial re-use, distribution, and reproduction in any medium, provided the original work is properly cited. For commercial re-use, please contact journals.permissions@oup.com

mechanistic target of rapamycin complex 1 (mTORC1) pathway, which regulates major functions such as protein synthesis and cell growth in response to cellular amino acid levels (14). Diseases caused by aberrant mTORC1 activation, such as tuberous sclerosis, are categorized as mTORopathies and are associated with epilepsy (15). *NPRL2* (HGNC#24969; OMIM# 607072) and *NPRL3* (HGNC#14124; OMIM#600928) are other subunits of the GATOR1 complex. Interestingly, autosomal dominant loss-of-function mutations in *NPRL2* and *NPRL3* were also identified in patients with focal epilepsies such as FFEVF, ADNFLE and FTLE (16,17), and they shared clinical features with patients with *DEPDC5*-related epilepsies (16–20). This suggests that the GATOR1 complex plays an important role in the pathogenesis of focal epilepsies. Variations in GATOR1 complex genes are more frequent and are associated with a broader spectrum of focal epilepsies compared with mTORopathies; they are conceptualized as a unique subset of mTORopathies, known as GATORopathies (21).

To decipher the mechanisms of GATORopathy, animal models recapitulating the clinical features of patients are essential. However, in contrast to *DEPDC5*, there are currently no animal models for *NPRL2*- and *NPRL3*-related epilepsies. Mice with germline knockout of *Nprl2* (*Nprl2*$^{-/-}$) or *Nprl3* (*Nprl3*$^{-/-}$) are embryonic lethal, similar to *Depdc5*$^{-/-}$ mice (22,23). *Nprl2*$^{-/-}$ mice had defective hematopoiesis, and *Nprl3*$^{-/-}$ mice showed cardiovascular defects. Heterozygous knockout (*Nprl2*$^{+/-}$ and *Nprl3*$^{+/-}$) rodents are viable, but their behavioral abnormality has not been evaluated. Muscle-specific *Nprl2* KO mice demonstrated altered fiber-type composition, resulting in abnormal running behavior (24). The knockdown of *Nprl3* in neuronal cell lines caused upregulation of mTORC1 activity and showed morphological alternation, soma enlargement and increased filopodia, which were reversed by an inhibitor of mTORC1, rapamycin (25).

Here, we conditionally deleted *Nprl2* and *Nprl3* from the dorsal telencephalon in mice [*Emx1*$^{cre/+}$;*Nprl2*$^{f/f}$ (*Nprl2*-cKO) and *Emx1*$^{cre/+}$;*Nprl3*$^{f/f}$ (*Nprl3*-cKO)] and compared their phenotypes with *Nprl2*$^{+/-}$, *Nprl3*$^{+/-}$ and *Emx1*$^{cre/+}$;*Depdc5*$^{f/f}$ (*Depdc5*-cKO) mice.

Results

Generation of floxed *Nprl2* and floxed *Nprl3* mice

To study the function of the *Nprl2* and *Nprl3* genes in epilepsy, we generated floxed *Nprl2* (*Nprl2*$^{f/f}$) and floxed *Nprl3* (*Nprl3*$^{f/f}$) mice by CRISPR-Cas9 genome editing technology using single-stranded DNA (ssDNA). We designed ssDNA donors and crispr RNAs (crRNAs) for *Nprl2* and *Nprl3* to knock-in *loxP* sites flanking targeted exons (Fig. 1A). We injected ssDNA, crRNA, trans-activating crispr RNA (tracrRNA) and Cas9 protein into mouse C57BL/6 embryos as previously reported (26) and confirmed that 53 and 71% of the delivered pups carried *loxP* sites in the targeted region of *Nprl2* and *Nprl3*, respectively, by Sanger sequencing (Supplementary Material, Table S1). Each founder mouse was backcrossed to wild-type C57BL/6 mice >6 times to eliminate potential off-target events.

Heterozygous germline *Nprl2*- and *Nprl3*-knockout mice did not show spontaneous seizures

Most heterozygous variations of *NPRL2* and *NPRL3* in patients with focal epilepsy are loss-of-function similar to *DEPDC5* variations (16,17,27). Thus, we generated heterozygous germline knockout *Nprl2* (*Nprl2*$^{+/-}$) and *Nprl3* (*Nprl3*$^{+/-}$) mice by crossing each floxed mice with B lymphocyte induced maturation protein 1 (*Blimp1*)-Cre mice expressing Cre recombinase in the primordial germ cells. Polymerase chain reaction (PCR) amplification of genomic DNA across the deleted region revealed that the intercross of the heterozygous KOs failed to generate homozygous KO mice, *Nprl2*$^{-/-}$ or *Nprl3*$^{-/-}$ mice (*Nprl2*, $P = 0.0238$; *Nprl3*, $P = 0.0421$; Chi-squared test) (Supplementary Material, Table S2). This suggests the occurrence of embryonic lethality, consistent with previous studies (22,23). Both *Nprl2*$^{+/-}$ ($n > 10$) and *Nprl3*$^{+/-}$ ($n > 10$) mice showed neither spontaneous seizures nor hyperactive behavior, such as wild running, under daily observation with routine handling over 1 year, similar to heterozygous germline *Depdc5*-knockout rodents (*Depdc5*$^{+/-}$) (8,9,11).

Generation of dorsal telencephalon-specific *Nprl2*-, *Nprl3*- and *Depdc5*-knockout mice

The *Emx1* (empty spiracles homeobox 1) gene is expressed in the dorsal telencephalon, which is the brain region commonly involved in epilepsy. In addition, *Depdc5* deletion in the dorsal telencephalon of mice, *Depdc5*$^{flox/flox}$-*Emx1*^{Cre} (*Depdc5*-*Emx1*-Cre cKO), recapitulates patient features, including spontaneous seizures and enlarged neurons (13). Thus, we crossed *Emx1*-Cre mice (*Emx1*$^{cre/+}$) (28,29) with each floxed mouse to obtain *Emx1*$^{cre/+}$; *Nprl2*$^{f/f}$ (*Nprl2*-cKO) and *Emx1*$^{cre/+}$; *Nprl3*$^{f/f}$ (*Nprl3*-cKO) mice. To compare the gene function among the GATOR1 subunits, we also generated *Emx1*$^{cre/+}$; *Depdc5*$^{f/f}$ (*Depdc5*-cKO) using *Depdc5*^{tm1c} (EUCOMM) Hmgu mice (referred to as *Depdc5*$^{f/f}$) containing *loxP* sites flanking exon 5 of *Depdc5* (12,13) (Fig. 1A). cKO mice of each GATOR1 subunit gene were born at the expected Mendelian ratio (*Depdc5*, $P = 0.6259$; *Nprl2*, $P = 0.9273$; *Nprl3*, $P = 0.8991$; Chi-squared test) (Supplementary Material, Table S3). Homozygous floxed mice for each gene (*Nprl2*$^{f/f}$, *Nprl3*$^{f/f}$ and *Depdc5*$^{f/f}$) were used as control mice in this study.

Cre-*loxP*-mediated recombination caused a deletion of exon 2–4 in *Nprl2*, resulting in a frame shift and premature stop codon at the 34th amino acid. In *Nprl3*, the recombination removed the 5′ UTR and the initiation codon of exon 1. To confirm reductions in the mRNA transcript of the KO genes, quantitative Reverse transcription PCR (RT-PCR) was performed using mRNAs extracted from the frontal cortex and cerebellum of each cKO and the control mice. Two sets of primers were designed

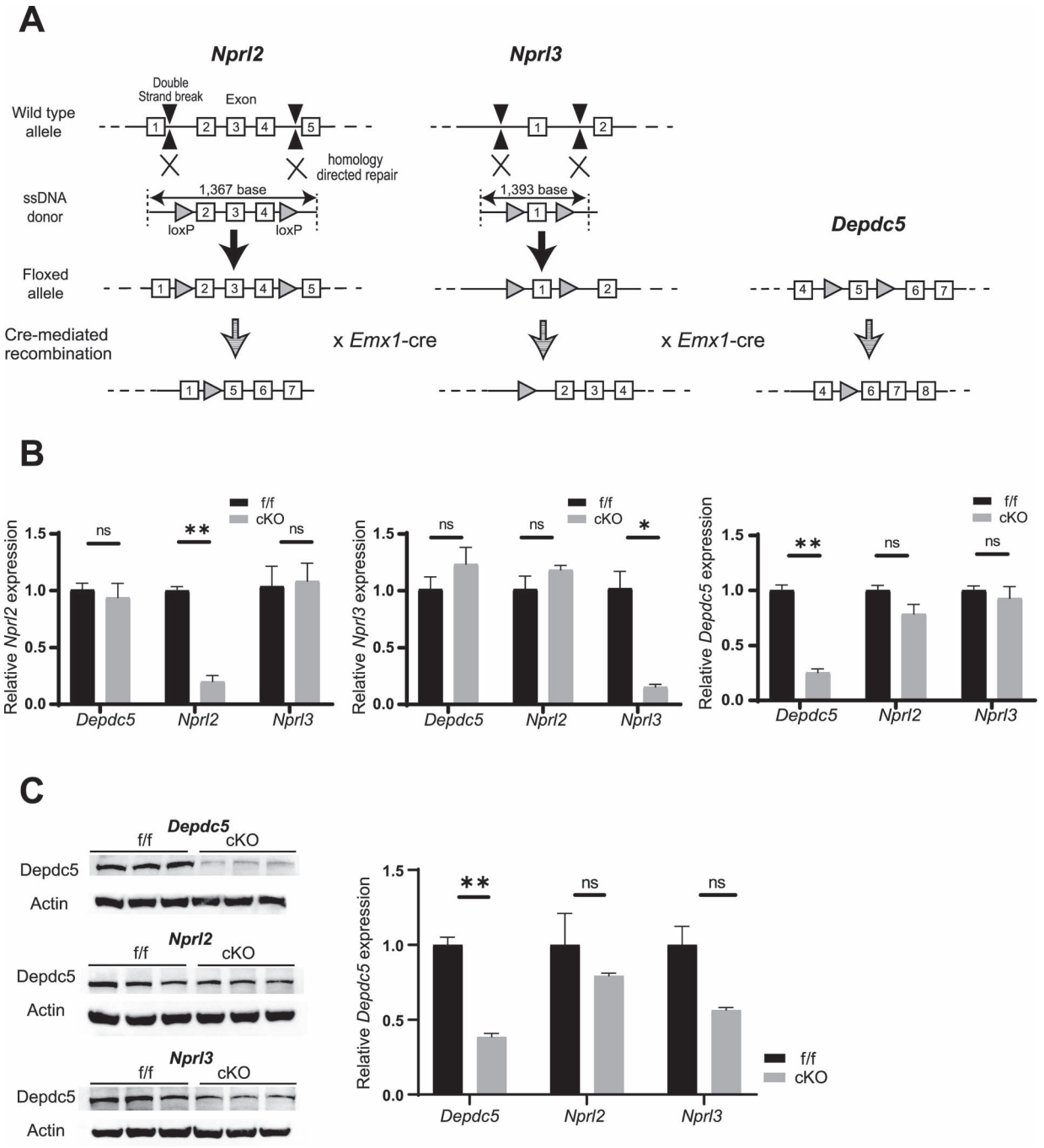

Figure 1. Generation of floxed *Nprl2* and floxed *Nprl3* mice and dorsal telencephalon-specific knockout mice of *Nprl2*, *Nprl3* and *Depdc5*. (**A**) Schematic illustration of the generation of $Nprl2^{f/f}$ and $Nprl3^{f/f}$ mice using the CRISPR-Ca9 system with ssDNA donors via homology directed repair mechanism. The Cre recombinase mediates site-specific recombination between two *loxP* sites. (**B**) Quantitative analysis of RT-PCR of *Nprl2*, *Nprl3* and *Depdc5* transcripts in the frontal cortex of P12 mice (f/f and cKO mice of GATOR1 subunit genes, $n = 3$ mice per genotype). Primer set 1 was used for the analysis. (**C**) Left panel: Representative western blots of cortical lysates derived from P12 mice (f/f and cKO mice of GATOR1 subunit genes, $n = 3$ mice per genotype) with Depdc5 and Actin antibodies. Right panel: histogram of densitometry analysis of Depdc5 normalized with Actin from left western blots. Graph error bars represent the mean ± SEM. $^*P < 0.05$; $^{**}P < 0.01$; ns: not significant, Student's *t*-test.

to amplify the coding sequence for each of *Nprl2* (ENSMUST00000010201.9), *Nprl3* (ENSMUST00000020530.12) and *Depdc5* (ENSMUST00000119705.8). Because Cre-mediated recombination is restricted to excitatory neurons and astrocytes in $Emx1^{cre/+}$ mice (28,30), the mRNA expression of each KO gene was not null. mRNA transcripts of the KO genes were significantly decreased in the frontal cortex of each cKO mouse compared with control mice (Fig. 1B, Supplementary Material, Fig. S1A), whereas the expression levels in the cerebellum were unchanged across the genotypes (Supplementary Material, Fig. S1B).

For the protein level, a significant reduction of Depdc5 in the cortex was confirmed in *Depdc5*-cKO mice compared with *Depdc5*-floxed mice by western blotting (Fig. 1C). Decreased Nprl2 and Nprl3 protein has

been previously reported in *Depdc5*^{Syn1} and *Depdc5*^{Emx1} (13,31) mice and iPSCs derived from patients with *DEPDC5* mutations (32). However, we failed to confirm the specificity of the anti-Nprl2 and Nprl3 antibodies used in these studies (Supplementary Material, Fig. S2). Thus, we could not confirm the reduction of Nprl2 and Nprl3 protein in Nprl2- and Nprl3-cKO mice.

The mTORC1 pathway was upregulated in the cerebral cortex of cKO mice

The GATOR1 complex prevents activation of the mTORC1 pathway; therefore, we examined mTOR activity by measuring the expression level of phosphorylated S6 (pS6), a downstream target of mTOR activation (8,10). Western blotting using cortical lysate from P12 pups revealed a significant increase in pS6 expression in *Nprl2*-, *Nprl3*- and *Depdc5*-cKO mice compared with control mice (Fig. 2A). No difference was observed in pS6 expression among these three cKO mouse strains [$P = 0.4789$, one-way analysis of variance (ANOVA)]. Decreased phosphorylated Akt (pAkt), representing compensatory feedback in response to hyperactivation of the mTORC1 pathway, was also shown in the three cKO mouse strains compared with control mice (Fig. 2A). The decrease of pAKT expression was smaller in *Nprl2*-cKO than in *Depdc5*- and *Nprl3*-cKO mice (*Nprl2*-cKO vs *Depdc5*-cKO, $P = 0.0144$; *Nprl2*-cKO vs *Nprl3*-cKO, $P = 0.0351$; *Depdc5*-cKO vs *Nprl3*-cKO, $P = 0.7315$, one-way ANOVA, Tukey's multiple comparison test). This suggests that the negative feedback loop was less active in *Nprl2*-cKO mice compared with *Nprl3*- and *Depdc5*-cKO mice.

The mTORC1 activity status was also evaluated by immunofluorescence staining. Intense pS6 signals were found in the cortex and hippocampus of all cKO mouse strains (Fig. 2B). Under the *Emx1* promoter, Cre recombinase is expressed in excitatory neurons and astrocytes in the dorsal telencephalon (30). However, the pS6 signal was colocalized with the neuronal marker, NeuN, but not with GFAP, an astrocyte marker (Fig. 2B). These results indicate that the mTORC1 pathway was upregulated in the cerebral cortex of these three cKO mouse strains.

Spontaneous seizures associated with premature death were observed in cKO mice

At birth, no noticeable difference in appearance was observed between mice of each cKO strain and their control littermates. However, from 2 weeks of age, *Nprl2*-, *Nprl3*- and *Depdc5*-cKO mice showed poor weight gain compared with control mice (Fig. 3A). This weight loss was accompanied by a decreased survival rate. Almost all cKO mice [*Depdc5*-cKO, 89% (8/9); *Nprl2*-cKO, 89% (8/9); *Nprl3*-cKO, 100% (9/9)] were dead by postnatal day (P)25 (Fig. 3B). One *Depdc5*-cKO mouse survived to P52 and one *Nprl2*-cKO mouse to P53.

Continuous non-invasive video recording during the second week after birth revealed all mice of each cKO mouse strain showed spontaneous hyperactive behavior, such as wild running, followed by generalized tonic–clonic seizure or clonic seizure ($n = 3$ for each genotype) (Videos S1–S3) and died either during seizure or in the recovery period. These results indicate that premature death in *Nprl2*-, *Nprl3*- and *Depdc5*-cKO mice is directly associated with seizures. No seizures or hyperactive behaviors were observed in control mice. Continuous video-electroencephalogram (EEG) recording (3 h/day) detected epileptiform discharges including spike-and-wave, polyspike and polyspike-and-wave discharges during seizures in each cKO mouse strain ($n = 3$ for each cKO strain) (Fig. 3C). Such discharge was not detected in control mice or during the interictal period in cKO mice. These results indicate that *Nprl2*-, *Nprl3*- and *Depdc5*-cKO mice share common phenotypic features of lethal epilepsy.

Megalencephaly and dysmorphic enlarged neurons were observed in cKO mice

Some epilepsy patients with GATOR1 subunit gene variations have cortical malformations such as FCD type 2 (6,17); therefore, we assessed the brains of 2-week-old *Nprl2*-, *Nprl3*- and *Depdc5*-cKO mice for morphological abnormalities.

NeuN immunostaining of coronal sections demonstrated increased thickness in *Nprl2*-, *Nprl3*- and *Depdc5*-cKO mice (Fig. 4A). In contrast, neuronal density was significantly decreased in the cortical layers in cKO mice (Fig. 4B). To investigate the etiology of the increased cortical thickness in these cKO mice, we measured the soma size of the neurons. We confirmed that the soma size of the NeuN-positive cells was significantly larger in *Nprl2*-, *Nprl3*- and *Depdc5*-cKO mice than in control mice (Fig. 4C). These neuropathological abnormalities in *Nprl2*-, *Nprl3*- and *Depdc5*-cKO mice, including megalencephaly and dysmorphic enlarged neuron size, recapitulated features of GATORopathy patients and were consistent with previous studies in mTORopathy mouse models (12,33,34).

Although rapamycin extends the lifespan of cKO mice, the benefit after withdrawal was less durable in *Nprl2*- and *Nprl3*-cKO mice compared with *Depdc5*-cKO mice

mTORC1 hyperactivity was observed in *Nprl2*-, *Nprl3*- and *Depdc5*-cKO mice; therefore, we examined whether chronic administration of the mTOR inhibitor, rapamycin, prevented premature death of *Nprl2*-, *Nprl3*- and *Depdc5*-cKO mice. Rapamycin (3 mg/kg) or vehicle was injected from P13 to P42 (5 days per week) as previously reported (13,33). Chronic rapamycin treatment dramatically decreased the expression of pS6 in *Nprl2*-, *Nprl3*- and *Depdc5*-cKO mice 5 days after the first injection (Supplementary Material, Fig. S3A). The chronic treatment significantly prolonged the lifespan of *Nprl2*-, *Nprl3*- and *Depdc5*-cKO mice compared with each vehicle-treated cKO mouse (Fig. 5A). Among the rapamycin-treated cKO mouse strains, there was no significant difference in

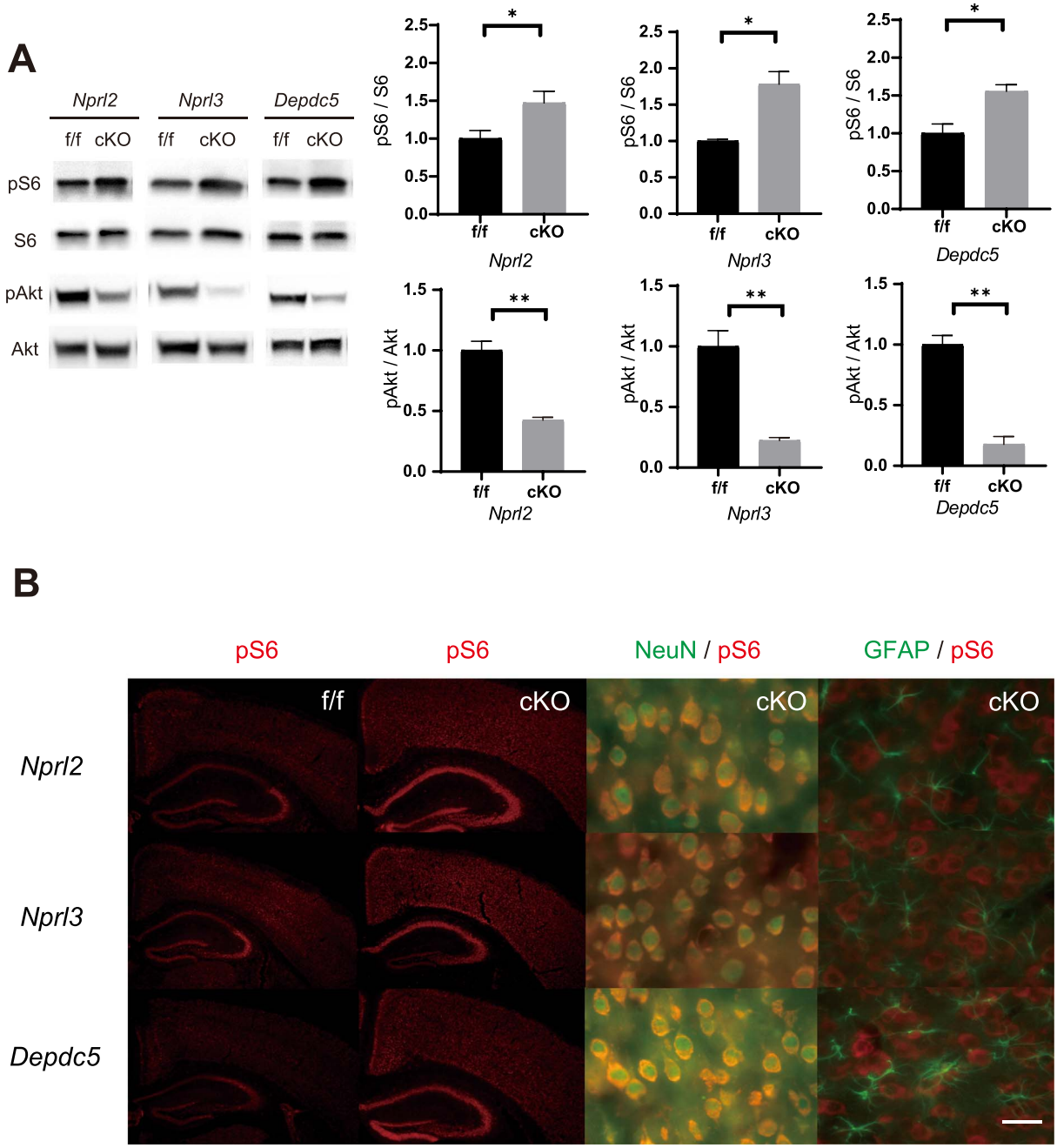

Figure 2. mTORC1 upregulation in cKO mice. (**A**) Left panel: Representative western blots of cortical lysates derived from P12 f/f and cKO mice of each GATOR1 subunit gene with pS6, S6, pAkt and Akt antibodies. Right panel: quantitative analysis of pS6 normalized with S6, and pAkt normalized with Akt ($n = 3$ mice per genotype). Graph error bars represent the mean ± SEM. *$P < 0.05$; **$P < 0.01$ (Student's *t*-test). (**B**) Representative immunostaining for pS6 protein (red), neuronal marker NeuN (green) and astrocyte marker GFAP (green) in a brain section from P12 f/f and cKO mice of each GATOR1 subunit gene. Scale bars: 500 μm (left and middle column), 25 μm (right column).

survival ratio [Log-rank (Mantel–Cox) test, $P = 0.1075$; Gehan–Breslow–Wilcoxon test, $P = 0.1374$].

We performed video recording to evaluate the seizure phenotype in cKO mouse strains treated with vehicle or rapamycin. Six-hour (3 h daytime, 3 h nighttime) continuous recording at 3–4 days after the first injection revealed a significant reduction in both the number and duration of generalized seizures in rapamycin-treated cKO mice compared with vehicle-treated cKO mice (Fig. 5B). There was no difference in the frequency and duration of generalized seizures among each rapamycin-treated cKO mouse strain (seizure frequency, $P = 0.1592$; seizure duration, $P = 0.0764$; one-way ANOVA). The effect of rapamycin on brain morphology was evaluated at P42 by immunohistochemistry and revealed increased cortical thickness and enlarged neuronal soma size in each cKO mouse strain compared with rapamycin-treated control mice (Supplementary Material, Fig. S3B). These findings indicate that chronic mTORC1 downregulation by rapamycin administration effectively inhibits seizure occurrence and the subsequent premature death, but not cortical malformation.

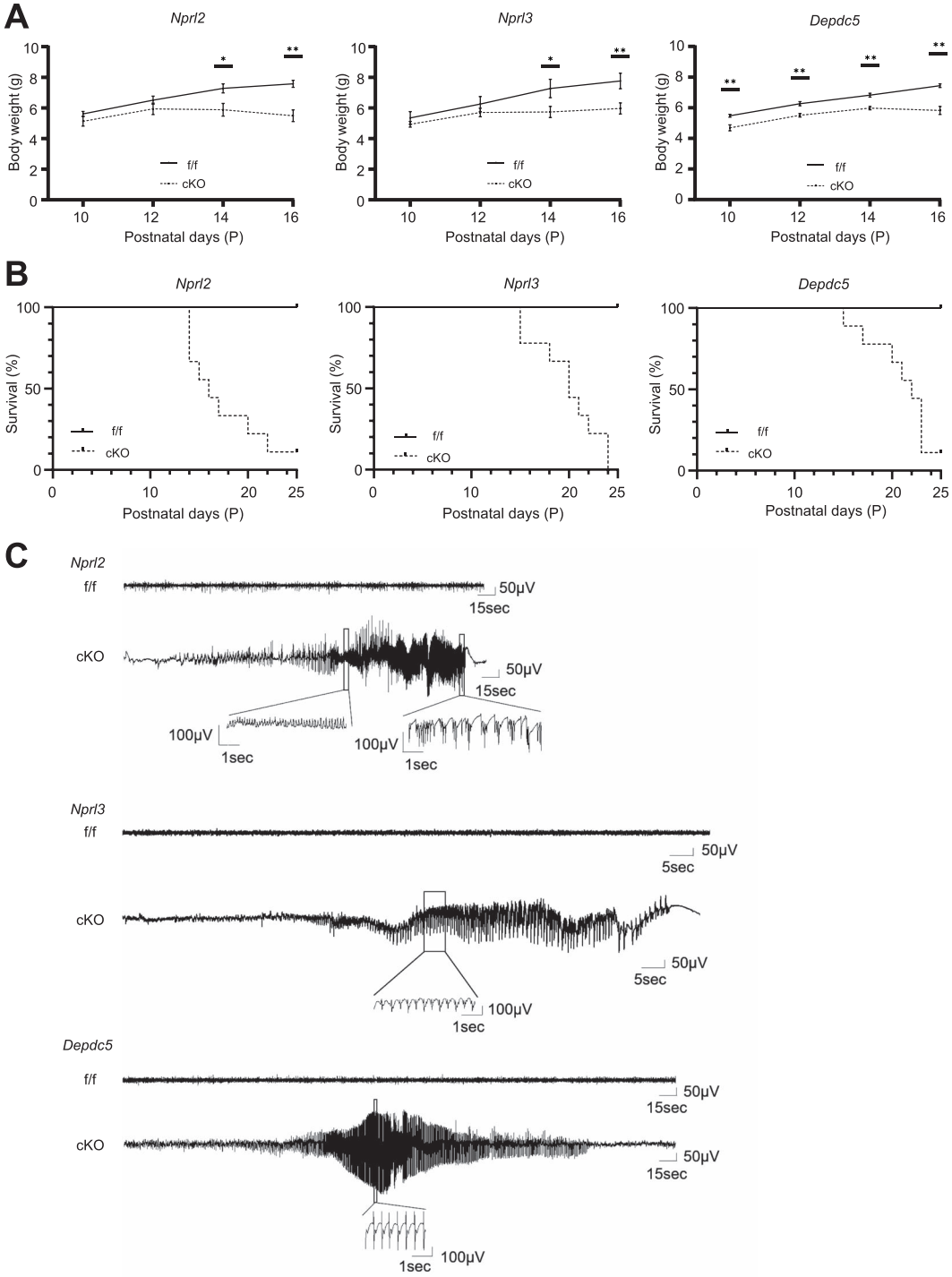

Figure 3. Spontaneous seizure associated with premature death in cKO mice. (**A**) Body weight of each floxed ($Nprl2^{f/f}$, $n = 8$; $Nprl3^{f/f}$, $n = 5$; $Depdc5^{f/f}$, $n = 7$) and cKO line (*Nprl2*-cKO, $n = 7$; *Nprl3*-cKO, $n = 9$; *Depdc5*-cKO, $n = 5$). Graph error bars represent the mean ± SEM. *$P < 0.05$; **$P < 0.01$ (Student's *t*-test). (**B**) Survival rate of each floxed and cKO line ($n = 9$ mice per genotype). $Nprl2^{f/f}$ versus *Nprl2* cKO, $P = 0.0001$; $Nprl3^{f/f}$ versus *Nprl3* cKO, $P < 0.0001$; $Depdc5^{f/f}$ versus *Depdc5* cKO, $P = 0.0002$ (Kaplan–Meier curves, log-rank test). (**C**) Representative EEG tracing of 2-week-old f/f and cKO mice of each GATOR1 subunit gene. Epileptiform discharges were recorded during generalized seizure in cKO mice.

A persistent benefit of rapamycin after withdrawal was observed in *Depdc5*-*Emx1*-Cre cKO mice (13). Consistent with this, 71% of *Depdc5*-cKO mice survived longer than P80 after withdrawal at P42 (Fig. 5C). However, all the *Nprl2*- and *Nprl3*-cKO mice died before P61, significantly earlier than *Depdc5*-cKO mice. Video recording revealed that all *Nprl2*- and *Nprl3*-cKO mice (*Nprl2*-cKO, $n = 3$; *Nprl3*-cKO, $n = 3$) died either during generalized seizures or in the recovery period after withdrawal at P42, similar to 2-week-old *Nprl2*- and *Nprl3*-cKO mice. Although significantly increased pS6 and decreased pAkt were observed 1 week after withdrawal of rapamycin (P49) (Fig. 5D), no significant difference was found in their expression among the three cKO mouse strains

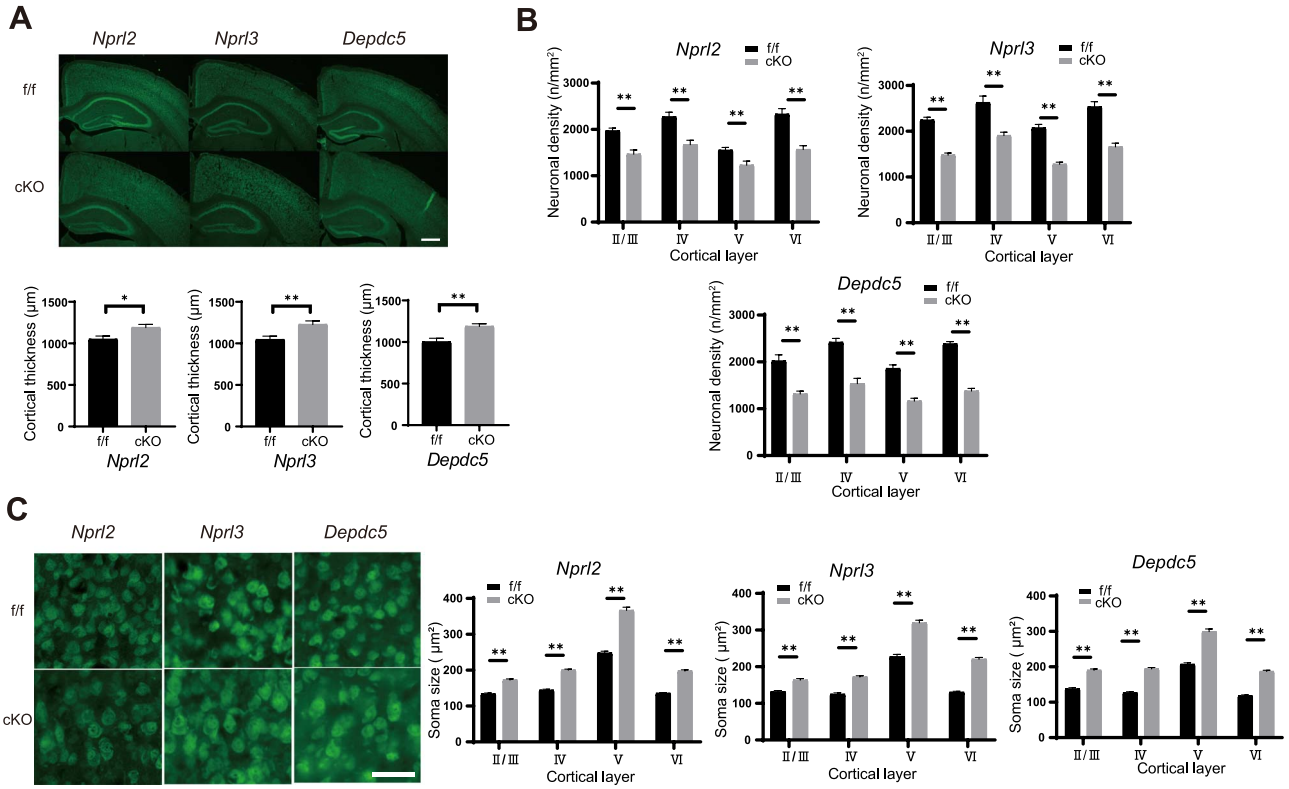

Figure 4. Neuropathological abnormalities in cKO mice. (**A**) Upper panel: Representative immunostaining patterns for neuronal marker, NeuN (green) in a brain section from 2-week-old f/f and cKO mouse of each GATOR1 subunit gene. Lower panel: Quantification of cortical thickness measured from six paired sites in three sections per brain ($n = 3$ mice per genotype). (**B**) Neuronal density measured from three paired areas of each layer in cortex ($n = 3$ mice per genotype). (**C**) Left panel: Representative immunostaining patterns for NeuN in a brain section. Right panel: Neuron soma size measured from 25 NeuN-positive cells in each layer ($n = 3$ mice per genotype). Scale bars: 500 μm for (A) and (C). Graph error bars represent the mean ± SEM. $^{*}P < 0.05$; $^{**}P < 0.01$ (Student's *t*-test).

(pS6, $P = 0.9097$; pAkt, $P = 0.3929$; one-way ANOVA). This suggests that mTORC1 activity is not directly associated with the reduced durability of the effect of rapamycin after withdrawal in *Nprl2*- and *Nprl3*-cKO mice.

Discussion

In this study, we demonstrated dorsal telencephalon-specific knockout of *Nprl2* and *Nprl3* in mice, as the first animal models of *NPRL2*- and *NPRL3*-related epilepsies. *Nprl2*- and *Nprl3*-cKO mice showed spontaneous seizures resulting in premature death. Although 67% of GATOR1 variations in epilepsy patients are heterozygous loss-of-function, *Nprl2*$^{+/-}$ and *Nprl3*$^{+/-}$ mice exhibited neither seizures nor hyperactive behavior during daily observation for >1 year, similar to *Depdc5*$^{+/-}$ rodents (8,9). This discrepancy can be explained either by species differences between humans and rodents or by a biallelic two-hit hypothesis.

Abnormal features of neuronal cells in the patients, such as increased soma size, were recapitulated in patient iPSC-derived cortical neurons harboring *Depdc5* mutations (32), but not in *Depdc5*$^{+/-}$ mouse models (9), suggesting the existence of species-specific differences (32).

Recent clinical studies reported the existence of somatic loss-of-function *DEPDC5* variations in brain specimens of focal epilepsy patients harboring *DEPDC5* germline variation (6,10). Because the somatic variation showed gradient expression around the seizure-onset zone (10), occurrence of the somatic variation resulted in biallelic inactivation (the somatic variation plus the germline variation) of *DEPDC5*, which is likely associated with the epileptogenesis. This two-hit hypothesis is also supported by animal models. Focal somatic inactivation of *Depdc5* in rodents (10,35) and conditional KO of *Depdc5* in mouse neuronal cells (*Depdc5*$^{flox/flox}$-*Syn1*^{Cre}) (12) and the dorsal telencephalon (*Depdc5*$^{flox/flox}$-*Emx1*^{Cre}) (13) result in spontaneous seizure (12,13,31). Interestingly, *Nprl2*- and *Nprl3*-cKO mice also share common phenotypic features with *Depdc5*-cKO mice. Although second-hit somatic variations have not yet been reported in *NPRL2* and *NPRL3* in patients, our results indicate that the two-hit hypothesis may also be applicable to *NPRL2*- and *NPRL3*-related epilepsies. Our results also show common effects of GATOR1 complex component loss, suggesting that there is no functional redundancy or compensation among the three subunits of the GATOR1 complex. These findings are also coincident with the fact that patients with *DEPDC5*, *NPRL2* or *NPRL3* mutations share common clinical features of focal epilepsies (21).

To evaluate the seizures of cKO mice, we performed video-EEG recording. Because they were pre-weaned, recording was performed for a limited period of up

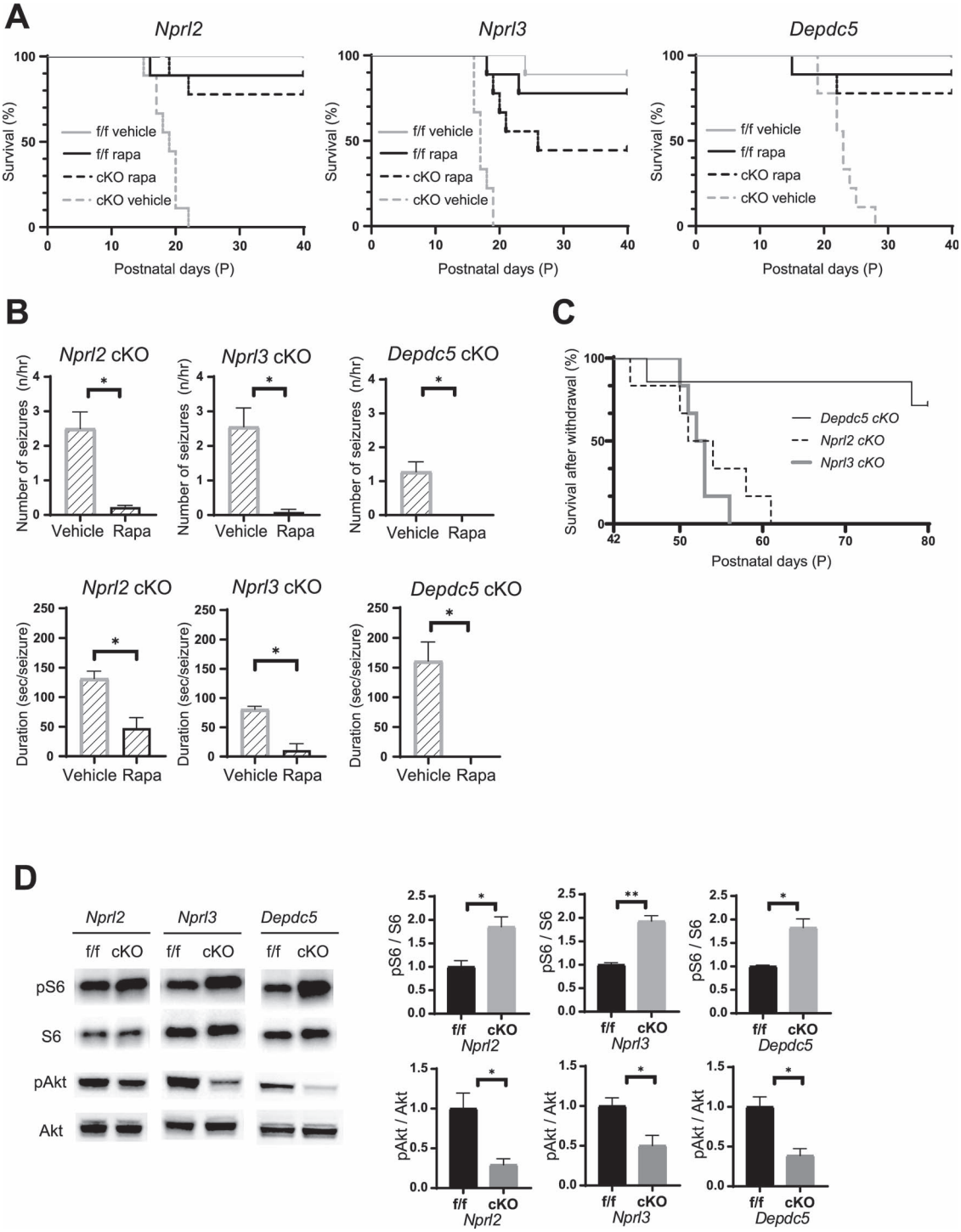

Figure 5. Chronic rapamycin administration extended the lifespan, but showed different outcomes after withdrawal among cKO mice. (**A**) Survival rate of f/f and cKO mice of GATOR1 subunit genes treated with vehicle or rapamycin (rapa) ($n = 9$ mice per group). *Nprl2*, cKO-vehicle vs cKO-rapa, $P = 0.0002$; *Nprl3*, cKO-vehicle vs cKO-rapa, $P = 0.0002$; *Depdc5*, cKO-vehicle vs cKO-rapa, $P = 0.0045$ (Kaplan–Meier curves, log-rank test). *Depdc5*-cKO-rapa vs *Nprl2*-cKO-rapa vs *Nprl3*-cKO-rapa, $P = 0.1075$ (Mantel–Cox, Log-rank test), $P = 0.1374$ (Gehan–Breslow–Wilcoxon test). (**B**) Number of generalized seizures (upper row) and duration of each seizure (lower row) observed for 6 h (3 h in daytime, 3 h in nighttime) in cKO mice of GATOR1 subunit genes treated with vehicle or rapamycin. (*Depdc5*, *Nprl2*, $n = 3$ each genotype; *Nprl3* f/f, $n = 3$; cKO, $n = 4$) $^*P < 0.05$, (one-tailed Mann–Whitney test). (**C**) Survival rate of *Depdc5*-cKO ($n = 7$), *Nprl2*-cKO ($n = 6$) and *Nprl3*-cKO ($n = 6$) mice after withdrawal of rapamycin administration. *Depdc5* cKO-rapa vs *Nprl2* cKO-rapa, $P = 0.0133$; *Depdc5* cKO-rapa vs *Nprl3* cKO-rapa, $P = 0.0212$; *Nprl2* cKO-rapa vs Nprl3 cKO-rapa, $P = 0.4391$ (Kaplan–Meier curves, log-rank test). (**D**) Left panel: Representative western blot of cortical lysates derived from P49 f/f and cKO mice of each GATOR1 subunit gene with pS6, S6, pAkt and Akt antibodies. Right panel: Quantitative analysis of pS6 normalized with S6, and pAkt normalized with Akt ($n = 3$ mice per genotype). $^*P < 0.05$; $^{**}P < 0.01$ (Student's *t*-test) Graph error bars represent the mean ± SEM.

to 3 h/day. Nevertheless, we detected typical epileptic discharges coinciding with the seizure. SUDEP occurs in 10% of patients with GATOR1 variations (7). SUDEP is defined as sudden, unexpected, witnessed or unwitnessed, non-traumatic or non-drowning death of people with epilepsy, with or without evidence of a seizure, excluding documented status epilepticus (SE) and in whom postmortem examination does not reveal a structural or toxicological cause for death (36). Because video-EEG recording was carried out for a limited period, we failed to detect an EEG at death. However, non-invasive long-term 24-h video recording revealed that all observed cKO mice died during generalized seizure or in the recovery period, including SE. It indicates that their death is strongly related to the occurrence of the seizure and may not be classified as SUDEP.

Mutations in GATOR1 subunit genes are also linked to focal epilepsies with malformation of cortical development such as FCD (17). Histopathological analysis of specimens from patients displayed enlarged and dysmorphic neurons with elevated mTORC1 activation as demonstrated by increased pS6 expression (4,10,17). We revealed that *Nprl2*- and *Nprl3*-cKO mice also demonstrated the same neuropathological abnormalities as patients, such as enlarged neuronal cells with increased pS6 signals, similar to *Depdc5*-cKO and other animal models of *Depdc5* (8,12,13). Because *Emx1* is expressed in neuroprogenitor cells of the dorsal telencephalon, Cre-dependent recombination occurs in the excitatory neurons and astrocytes of the dorsal telencephalon. However, an intense pS6 signal was detected only in neuronal cells, not in astrocytes, by immunohistochemistry (Fig. 2B). Klofas *et al*. (13) showed hyperactivation of mTORC1 in cultured primary astrocytes of *Depdc5*-*Emx1*-Cre cKO mice. Although a significant increase of pS6 was confirmed in cultured astrocytes by western blotting, the extent of the increase was much smaller compared with that in the whole cortical lysate. In our immunofluorescence images, pS6 signals in astrocytes may be masked by the intense pS6 signal in neuronal cells. Further experiments using astrocyte primary culture will be necessary to determine the expression of *Nprl2* and *Nprl3* in astrocytes, in addition to mTOR activity in the cells.

Thirty percent of the probands of GATOR1-related epilepsy had early-onset epilepsy (7). This means that the GATOR1 genes are crucial for proper brain development, and their defect may result in disruption of neuronal connections and seizure. In mice, the period of intense synaptogenesis is limited to the first 2 weeks after birth (37). Chronic administration of the mTOR inhibitor rapamycin from P13 improved survival in *Nprl2*- and *Nprl3*-cKO mice compared with each vehicle-treated cKO mouse. Video recording revealed that the number and duration of generalized seizures significantly decreased in rapamycin-treated cKO mice. This result indicates that mTORC1 pathway hyperactivation is involved in epilepsy development in *Nprl2*- and *Nprl3*-cKO mice. It also suggests that postnatal rapamycin treatment may be effective for the treatment of GATORopathy seizures.

In contrast, our study revealed different durabilities of the rapamycin effect after withdrawal among GATOR1 cKO mice. As previously reported (13), the effect of rapamycin was durable in our *Depdc5*-cKO mice even after withdrawal at P42. They survived longer than P80. However, all the observed *Nprl2*- and *Nprl3*-cKO mice exhibited recurrent generalized seizures and died by P61 after withdrawal of rapamycin at P42. Because the increased expression of pS6 1 week after withdrawal was equivalent among the three cKO mouse strains, the phenotypic difference may be independent from the mTORC1 activation level at that time. Similar to our *Nprl3*-cKO mice, a recent medical case report showed that chronic treatment with the mTORC1 inhibitor sirolimus for 3.5 months completely inhibited the seizures of a patient with *NPRL3* mutation, but seizures reoccurred after 1 week of withdrawal (19). In another report, sirolimus given for 17 days with adequate serum drug level failed to control the seizures of a patient with *NPRL3* mutation (20). Because mTORC1 inhibitors are expected to be a potential targeted treatment for GATOR1 epilepsy, further comparative studies using *Depdc5*-, *Nprl2*- and *Nprl3*-cKO mice may be important to reveal the mechanism of the different rapamycin treatment outcomes. Transcriptome analysis, such as RNA-seq, using these three cKO mouse strains, will facilitate identification of the common and different genetic players for each related epilepsy and the understanding of GATORopathy. It will also contribute to the identification of new drug targets.

In summary, here we generated the first epileptic animal model of *NPRL2*- and *NPRL3*-related epilepsies as novel animal models of GATORopathies. Dorsal telencephalon-specific conditional knockout of *Nprl2* and *Nprl3* in mice identically recapitulated the major abnormal features of the patients, spontaneous seizures and dysmorphic enlarged neuronal cells with increased mTORC1 signaling. Because no seizures were observed in heterozygous *Nprl2*- or *Nprl3*-knockout mice, our results propose a 'two-hit' hypothesis for the pathogenesis of *NPRL2*- and *NPRL3*-related epilepsies. Although chronic postnatal rapamycin administration dramatically inhibited seizure occurrence and prolonged the survival period, the benefit of rapamycin administration was significantly less durable after withdrawal in *Nprl2*- and *Nprl3*-cKO mice compared with *Depdc5*-cKO mice. Further detailed comparative studies using *Nprl2*-, *Nprl3*- and *Depdc5*-cKO mice will facilitate the understanding of the underlying pathogenic mechanisms and the genetic architecture of GATORopathy.

Materials and Methods

Mice

To generate floxed *Nprl2* (*Nprl2*$^{f/f}$) and floxed *Nprl3* (*Nprl3*$^{f/f}$) mice using the CRISPR-Cas9 system, ssDNA composed of the targeted exon flanked by two *loxP*

sites was injected into C57BL/6 mouse zygotes with crRNA, tracrRNA and Cas9 Protein as previously reported (26,38). The ssDNA, crRNA and tracrRNA were provided by Fasmac (Kanagawa, Japan). The nucleotide sequences used are listed in Supplementary Material, Table S4. Both floxed mice, *Nprl2*$^{f/f}$ and *Nprl3*$^{f/f}$, and heterozygous KO mice, *Nprl2*$^{+/-}$ and *Nprl3*$^{+/-}$, were deposited with the National Bio Resource Project for the Mouse in Japan. Genomic DNA was extracted from tail biopsies. Primers used for genotyping are listed in Supplementary Material, Table S5. Floxed *Depdc5* mice (*Depdc5*$^{tm1c(EUCOMM)Hmgu}$, referred to as *Depdc5*$^{f/f}$) and *Emx1*-Cre mice (*Emx1*$^{cre/+}$) (29) were obtained from the MRC Harwell Institute and the RIKEN BioResource Center, respectively. *Blimp1*-Cre mice were kindly provided by Dr Takahiro Adachi (Tokyo Medical and Dental University, Tokyo, Japan).

All animal care and experimental procedures were approved by the Institutional Animal Care and Use Committee of Tokyo Medical and Dental University. Mice were maintained in a 12-h light/dark cycle with food and water ad libitum.

Quantitative reverse transcription PCR analysis

RNA was extracted from the frontal cortex and cerebellum of mice using a RNeasy Plus Universal Mini Kit (QIAGEN, Hilden, Germany) or Maxwell Rapid Sample Concentrator Instrument (Promega, Madison, WI, USA). One μg of each RNA sample was subjected to reverse transcription using the Prime Script RT reagent kit (Takara Bio, Shiga, Japan). Quantitative PCR was performed using SsoAdvanced Universal SYBR Green Supermix (Bio-Rad) on a CFX connect/CFX96 Deep Well Real-Time PCR Detection System (Bio-Rad). All primer sets used for quantitative PCR are listed in Supplementary Material, Table S5. The Δ cycle threshold (ΔCt) values were calculated as the mean Ct for the target gene, *Nprl2* and *Nprl3*, minus the mean Ct for the control gene, *Gapdh*. The fold differential expression of the target gene in tissues of cKO mice compared with that of floxed mice was expressed as $2^{-\Delta\Delta Ct}$ and analyzed as previously reported (12).

Western blotting

Brain samples of mice were flash-frozen in liquid nitrogen and homogenized using an ultrasonic homogenizer in 2 × cell lysis buffer (Cell signaling, Danvers, MA, USA) supplemented with phosphatase inhibitor PhosSTOP (Sigma-Aldrich, St. Louis, MO, USA) and complete protease inhibitor (Sigma-Aldrich), according to the manufacturer's instructions. Total protein samples (35 μg) were separated on 4–15% gradient sodium dodecyl sulfate (SDS)-polyacrylamide gels (Bio-Rad, Hercules, CA, USA) and 4–12% Bolt™ Bis-Tris Plus gels (Thermo Fisher, Waltham, MA, USA) and transferred to polyvinylidene difluoride membranes (Bio-Rad/Thermo Fisher). The primary antibodies used were as follows: anti-Depdc5 (Abcam, Cambridge, UK, #ab185565, 1:1000), anti-βactin (8H10D10) (Cell signaling, #3700, 1:2000), anti-phospho-S6 Ribosomal Protein (Ser 240/244) (Cell signaling, #5364, 1:1000), anti-S6 Ribosomal Protein (Cell signaling, #14467, 1:1000), anti-phospho-Akt (ser473) (Cell signaling, #4060, 1:2000) and Akt (pan) (Cell signaling #2920, 1:2000). Signals were detected by chemiluminescence using ImageLab (Bio-Rad) and iBright CL 1500 (Thermo Fisher).

Immunohistochemistry

Mice were deeply anesthetized and transcardially perfused with 4% paraformaldehyde (PFA) in phosphate-buffered saline (PBS). After the brains were removed, they were postfixed in 4% PFA at 4°C overnight and then cryoprotected in 30% sucrose/0.1 M PBS. Brain sections 35 μm thick were prepared using a cryostat (Leica, Wetzlar, Germany). Immunostaining experiments were performed as previously reported (8). The primary antibodies used were anti-NeuN (Millipore, Burlington, MA, USA, #MAB377), anti-GFAP (GA5) (Cell signaling, #3670) and anti-phospho-S6 Ribosomal Protein (Ser 240/244) (Cell signaling, #5364). Primary antibodies were detected with the following secondary antibodies: donkey anti-rabbit IgG (H + L) highly cross-adsorbed secondary antibody, Alexa Fluor 568 (Invitrogen, Carlsbad, CA, USA) and donkey anti-mouse IgG (H + L) highly cross-adsorbed secondary antibody, Alexa Fluor 488 (Invitrogen). Images were acquired using a BZ-X700 fluorescence microscope (KEYENCE, Osaka, Japan) and BZ-X-Analyzer software (KEYENCE).

Cortical thickness, neuron density and neuron soma size of mice were measured using ImageJ software. Three anatomically matched sections per mouse were used from the three cKO mouse lines and three floxed mouse lines. Cortical thickness was measured from six locations per section. The measurement of neuron soma size was performed for 25 neuronal cells at each layer per section for 2-week-old samples and at layer V per section for P42 samples as previously reported (12). The analysis was carried out blind with respect to genotype.

Video-EEG recording

For implantation of EEG electrodes, 2-week-old mice were anesthetized with isoflurane and fixed in a stereotaxic instrument. Small holes were made in the skull, and screw electrodes (#SNZS-M1-3; NBK, Gifu, Japan) for EEG recording were placed on the surface of the frontal cortex. The reference electrode was implanted on the right frontal cranium. All electrodes were soldered to a connector and fixed to the skull with dental cement. After a recovery period of at least 1 day, mice were placed individually in a chamber equipped with a video-EEG recording system. Because the mice had not been weaned, video-EEG recording was performed for up to 3 h per day. The visual recorder, AQ-VU (TEAC, Tokyo, Japan), was used to store video taken from the above and from the side. Continuous EEG was recorded using an amplifier (HAS-4; Bio Research Center, Nagoya, Japan). The recorded EEG signals were stored and analyzed using Lab chart software (AD Instruments, Sydney, Australia).

Rapamycin treatment

Rapamycin treatment was performed as previously reported (13,33). Rapamycin (LC Laboratories, Woburn, MA, USA) was dissolved at 30 mg/ml in ethanol and stored at −20°C as a stock solution. This was diluted with vehicle (0.25% Tween-20/0.25% polyethylene glycol) in PBS. Rapamycin (3 mg/kg) or vehicle was intraperitoneally injected into cKO and floxed mice 5 days per week, Monday–Friday, from P13–42.

During the injection period, cKO mice at an age between P15 and P20 were monitored with their mothers by a non-invasive video recording system (O'Hara & Co., Ltd, Tokyo, Japan) under a standard 12-h bright–dark cycle and ad libitum access to water and food. Frequency and duration of generalized seizures, including tonic, clonic and tonic–clonic seizures, were determined by observers blinded to both treatment and genotype. Recorded videos used for analysis were randomly chosen (total 6 h: 3 h light on, 3 h light off).

Statistical analysis

Statistical analysis was performed using GraphPad Prism 8 software (GraphPad, San Diego, CA, USA). The results are presented as the mean ± SEM. Comparisons between two groups were performed by unpaired two-tailed Student's *t*-test for parametric data, two-tailed Student's *t*-test with Welch's correction if SDs were not equal, and the Mann–Whitney test was conducted for non-parametric data. Comparisons among multiple groups were analyzed by ordinary one-way ANOVA with Tukey's multiple comparison test or two-way ANOVA with Sidak's multiple comparison test as *post hoc* analysis for parametric data. A log-rank (Mantel–Cox) test was used to compare the Kaplan–Meier analysis for survival distribution.

Supplementary Material

Supplementary Material is available at *HMG* online.

Acknowledgements

The authors thank Michiko Nakagawa, Harumi Ishikubo and Takako Usami for technical support, and Yusaku Wada (Fasmac) for providing technical assistance and materials.

Conflict of Interest statement. None declared.

Funding

Japan Society for the Promotion of Science KAKENHI (JP 16H06765, JP 18K14608, JP 21K05987); Ichiro Kanehara Foundation for the Promotion of Medical Sciences and Medical Care.

References

1. Devinsky, O., Vezzani, A., O'Brien, T.J., Jette, N., Scheffer, I.E., de Curtis, M. and Perucca, P. (2018) Epilepsy. *Nat. Rev. Dis. Primers.*, **4**, 1–24.
2. Dibbens, L.M., de Vries, B., Donatello, S., Heron, S.E., Hodgson, B.L., Chintawar, S., Crompton, D.E., Hughes, J.N., Bellows, S.T., Klein, K.M. *et al.* (2013) Mutations in DEPDC5 cause familial focal epilepsy with variable foci. *Nat. Genet.*, **45**, 546–551.
3. Ishida, S., Picard, F., Rudolf, G., Noé, E., Achaz, G., Thomas, P., Genton, P., Mundwiller, E., Wolff, M., Marescaux, C. *et al.* (2013) Mutations of DEPDC5 cause autosomal dominant focal epilepsies. *Nat. Genet.*, **45**, 552–555.
4. Scerri, T., Riseley, J.R., Gillies, G., Pope, K., Burgess, R., Mandelstam, S.A., Dibbens, L., Chow, C.W., Maixner, W., Harvey, A.S. *et al.* (2015) Familial cortical dysplasia type IIA caused by a germline mutation in DEPDC5. *Ann. Clin. Transl. Neurol.*, **2**, 575–580.
5. Cen, Z., Guo, Y., Lou, Y., Jiang, B., Wang, J. and Feng, J. (2017) De novo mutation in DEPDC5 associated with unilateral pachygyria and intractable epilepsy. *Seizure*, **50**, 1–3.
6. Baulac, S., Ishida, S., Marsan, E., Miquel, C., Biraben, A., Nguyen, D.K., Nordli, D., Cossette, P., Nguyen, S., Lambrecq, V. *et al.* (2015) Familial focal epilepsy with focal cortical dysplasia due to DEPDC5 mutations. *Ann. Neurol.*, **77**, 675–683.
7. Baldassari, S., Picard, F., Verbeek, N.E., van Kempen, M., Brilstra, E.H., Lesca, G., Conti, V., Guerrini, R., Bisulli, F., Licchetta, L. *et al.* (2019) The landscape of epilepsy-related GATOR1 variants. *Genet. Med.*, **21**, 398–408.
8. Marsan, E., Ishida, S., Schramm, A., Weckhuysen, S., Muraca, G., Lecas, S., Liang, N., Treins, C., Pende, M., Roussel, D. *et al.* (2016) Depdc5 knockout rat: a novel model of mTORopathy. *Neurobiol. Dis.*, **89**, 180–189.
9. Hughes, J., Dawson, R., Tea, M., McAninch, D., Piltz, S., Jackson, D., Stewart, L., Ricos, M.G., Dibbens, L.M., Harvey, N.L. *et al.* (2017) Knockout of the epilepsy gene Depdc5 in mice causes severe embryonic dysmorphology with hyperactivity of mTORC1 signalling. *Sci. Rep.*, **7**, 12618.
10. Ribierre, T., Deleuze, C., Bacq, A., Baldassari, S., Marsan, E., Chipaux, M., Muraca, G., Roussel, D., Navarro, V., Leguern, E. *et al.* (2018) Second-hit mosaic mutation in mTORC1 repressor DEPDC5 causes focal cortical dysplasia-associated epilepsy. *J. Clin. Invest.*, **128**, 2452–2458.
11. De Fusco, A., Cerullo, M.S., Marte, A., Michetti, C., Romei, A., Castroflorio, E., Baulac, S. and Benfenati, F. (2020) Acute knockdown of Depdc5 leads to synaptic defects in mTOR-related epileptogenesis. *Neurobiol. Dis.*, **139**, 104822.
12. Yuskaitis, C.J., Jones, B.M., Wolfson, R.L., Super, C.E., Dhamne, S.C., Rotenberg, A., Sabatini, D.M., Sahin, M. and Poduri, A. (2018) A mouse model of DEPDC5-related epilepsy: neuronal loss of Depdc5 causes dysplastic and ectopic neurons, increased mTOR signaling, and seizure susceptibility. *Neurobiol. Dis.*, **111**, 91–101.
13. Klofas, L.K., Short, B.P., Zhou, C. and Carson, R.P. (2020) Prevention of premature death and seizures in a Depdc5 mouse epilepsy model through inhibition of mTORC1. *Hum. Mol. Genet.*, **29**, 1365–1377.
14. Laplante, M. and Sabatini, D.M. (2012) mTOR signaling in growth control and disease. *Cell*, **149**, 274–293.
15. Crino, P.B. (2015) mTOR Signaling in epilepsy: insights from malformations of cortical development. *Cold Spring Harb. Perspect. Med.*, **5**, a022442.
16. Ricos, M.G., Hodgson, B.L., Pippucci, T., Saidin, A., Ong, Y.S., Heron, S.E., Licchetta, L., Bisulli, F., Bayly, M.A., Hughes, J. *et al.* (2016) Mutations in the mammalian target of rapamycin pathway regulators NPRL2 and NPRL3 cause focal epilepsy. *Ann. Neurol.*, **79**, 120–131.
17. Weckhuysen, S., Marsan, E., Lambrecq, V., Marchal, C., Morin-Brureau, M., An-Gourfinkel, I., Baulac, M., Fohlen, M., Zetchi, C.K.,

Seeck, M. *et al.* (2016) Involvement of GATOR complex genes in familial focal epilepsies and focal cortical dysplasia. *Epilepsia*, **57**, 994–1003.
18. Benova, B., Sanders, M.W.C.B., Uhrova-Meszarosova, A., Belohlavkova, A., Hermanovska, B., Novak, V., Stanek, D., Vlckova, M., Zamecnik, J., Aronica, E. *et al.* (2021) GATOR1-related focal cortical dysplasia in epilepsy surgery patients and their families: a possible gradient in severity? *Eur. J. Paediatr. Neurol.*, **30**, 88–96.
19. Vawter-Lee, M., Franz, D.N., Fuller, C.E. and Greiner, H.M. (2019) Clinical letter: a case report of targeted therapy with sirolimus for NPRL3 epilepsy. *Seizure*, **73**, 43–45.
20. Chandrasekar, I., Tourney, A., Loo, K., Carmichael, J., James, K., Ellsworth, K.A., Dimmock, D. and Joseph, M. (2021) Hemimegalencephaly and intractable seizures associated with the NPRL3 gene variant in a newborn: a case report. *Am. J. Med. Genet. A*, **185**, 2126–2130.
21. Iffland, P.H., Carson, V., Bordey, A. and Crino, P.B. (2019) GATORopathies: the role of amino acid regulatory gene mutations in epilepsy and cortical malformations. *Epilepsia*, **60**, 2163–2173.
22. Dutchak, P.A., Laxman, S., Estill, S.J., Wang, C., Wang, Y., Wang, Y., Bulut, G.B., Gao, J., Huang, L.J. and Tu, B.P. (2015) Regulation of hematopoiesis and methionine homeostasis by mTORC1 inhibitor NPRL2. *Cell Rep.*, **12**, 371–379.
23. Kowalczyk, M.S., Hughes, J.R., Babbs, C., Sanchez-Pulido, L., Szumska, D., Sharpe, J.A., Sloane-Stanley, J.A., Morriss-Kay, G.M., Smoot, L.B., Roberts, A.E. *et al.* (2012) Nprl3 is required for normal development of the cardiovascular system. *Mamm. Genome*, **23**, 404–415.
24. Dutchak, P.A., Estill-Terpack, S.J., Plec, A.A., Zhao, X., Yang, C., Chen, J., Ko, B., Deberardinis, R.J., Yu, Y. and Tu, B.P. (2018) Loss of a negative regulator of mTORC1 induces aerobic glycolysis and altered Fiber composition in skeletal muscle. *Cell Rep.*, **23**, 1907–1914.
25. Iffland, P.H., Baybis, M., Barnes, A.E., Leventer, R.J., Lockhart, P.J. and Crino, P.B. (2018) DEPDC5 and NPRL3 modulate cell size, filopodial outgrowth, and localization of mTOR in neural progenitor cells and neurons. *Neurobiol. Dis.*, **114**, 184–193.
26. Aida, T., Chiyo, K., Usami, T., Ishikubo, H., Imahashi, R., Wada, Y., Tanaka, K.F., Sakuma, T., Yamamoto, T. and Tanaka, K. (2015) Cloning-free CRISPR/Cas system facilitates functional cassette knock-in in mice. *Genome Biol.*, **16**, 87.
27. Sim, J.C., Scerri, T., Fanjul-Fernández, M., Riseley, J.R., Gillies, G., Pope, K., van Roozendaal, H., Heng, J.I., Mandelstam, S.A., McGillivray, G. *et al.* (2016) Familial cortical dysplasia caused by mutation in the mammalian target of rapamycin regulator NPRL3. *Ann. Neurol.*, **79**, 132–137.
28. Gorski, J.A., Talley, T., Qiu, M., Puelles, L., Rubenstein, J.L.R. and Jones, K.R. (2002) Cortical excitatory neurons and glia, but not GABAergic neurons, are produced in the Emx1-expressing lineage. *J. Neurosci.*, **22**, 6309–6314.
29. Iwasato, T., Datwani, A., Wolf, A.M., Nishiyama, H., Taguchi, Y., Tonegawa, S., Knöpfel, T., Erzurumlu, R.S. and Itohara, S. (2000) Cortex-restricted disruption of NMDAR1 impairs neuronal patterns in the barrel cortex. *Nature*, **406**, 726–731.
30. Iwasato, T., Nomura, R., Ando, R., Ikeda, T., Tanaka, M. and Itohara, S. (2004) Dorsal telencephalon-specific expression of Cre recombinase in PAC transgenic mice. *Genesis*, **38**, 130–138.
31. Yuskaitis, C.J., Rossitto, L.-A., Gurnani, S., Bainbridge, E., Poduri, A. and Sahin, M. (2019) Chronic mTORC1 inhibition rescues behavioral and biochemical deficits resulting from neuronal Depdc5 loss in mice. *Hum. Mol. Genet.*, **28**, 2952–2964.
32. Klofas, L.K., Short, B.P., Snow, J.P., Sinnaeve, J., Rushing, G.V., Westlake, G., Weinstein, W., Ihrie, R.A., Ess, K.C. and Carson, R.P. (2020) DEPDC5 haploinsufficiency drives increased mTORC1 signaling and abnormal morphology in human iPSC-derived cortical neurons. *Neurobiol. Dis.*, **143**, 104975.
33. Carson, R.P., Van Nielen, D.L., Winzenburger, P.A. and Ess, K.C. (2012) Neuronal and glia abnormalities in Tsc1-deficient forebrain and partial rescue by rapamycin. *Neurobiol. Dis.*, **45**, 369–380.
34. Kassai, H., Sugaya, Y., Noda, S., Nakao, K., Maeda, T., Kano, M. and Aiba, A. (2014) Selective activation of mTORC1 Signaling recapitulates microcephaly, tuberous sclerosis, and neurodegenerative diseases. *Cell Rep.*, **7**, 1626–1639.
35. Hu, S., Knowlton, R.C., Watson, B.O., Glanowska, K.M., Murphy, G.G., Parent, J.M. and Wang, Y. (2018) Somatic Depdc5 deletion recapitulates electroclinical features of human focal cortical dysplasia type IIA. *Ann. Neurol.*, **84**, 140–146.
36. Maguire, M.J., Jackson, C.F., Marson, A.G. and Nevitt, S.J. (2020) Treatments for the prevention of sudden unexpected death in epilepsy (SUDEP). *Cochrane Database Syst. Rev.*, **4**, CD011792.
37. Chen, V.S., Morrison, J.P., Southwell, M.F., Foley, J.F., Bolon, B. and Elmore, S.A. (2017) Histology atlas of the developing prenatal and postnatal mouse central nervous system, with emphasis on prenatal days E7.5 to E18.5. *Toxicol. Pathol.*, **45**, 705–744.
38. Miyasaka, Y., Uno, Y., Yoshimi, K., Kunihiro, Y., Yoshimura, T., Tanaka, T., Ishikubo, H., Hiraoka, Y., Takemoto, N., Tanaka, T. *et al.* (2018) CLICK: one-step generation of conditional knockout mice. *BMC Genomics*, **19**, 318.